#6445

Building and Environment, Vol. 27, No. 3, pp. 387–397, 1992.
Printed in Great Britain.

0360–1323/92 $5.00+0.00

Prediction of Moisture Transfer in Building Constructions

CARSTEN RODE PEDERSEN*

Existing methods available for practising designers and architects to calculate moisture transfer through building constructions are reviewed and a transient model for combined heat and moisture transfer in composite constructions is introduced. Results using the transient model on a particular case are compared with those obtained using the traditional methods. The consideration of hygroscopic inertia by the transient model significantly alters the prediction of how moisture migrates within and through a building construction.

NOMENCLATURE

- c_p specific heat capacity, J/(kg · K)
- E solar irradiance, W/m²
- f displacement factor,-
- g moisture flux, kg/(m² · s)
- h heat transfer coefficient, W/(m² · K)
- h specific enthalpy (with respect to dry mass), J/kg
- Δh enthalpy of phase change, J/kg
- K hydraulic conductivity, kg/(m · s · Pa)
- P liquid pressure, Pa
- p partial pressure of water vapour, Pa
- q heat flux, W/m²
- R thermal resistance, m² · K/W
- R_v gas constant for water vapour, J/(kg · K)
- T temperature, K
- t time, s
- U overall heat transfer coefficient, W/(m² · K)
- u moisture content, kg/kg
- v wind speed, m/s
- x one dimensional space co-ordinate, m
- Z vapour resistance, m² · s · Pa/kg
- α absorptance,-
- β convective mass transfer coefficient, kg/(m² · s · Pa)
- δ vapour permeability, kg/(m · s · Pa)
- ε emissivity,-
- λ thermal conductivity, W/(m · K)
- Ξ moisture capacity in the suction diagram,-
- ξ moisture capacity in the sorption diagram,-
- ρ density, kg/m³
- σ Stefan–Boltzmann constant, W/(m² · K⁴)
- φ relative humidity,-

Numerical Functions

- H_q heat transfer coefficient, W/(m² · K)
- H_v vapour transfer coefficient, kg/(m² · s · Pa)
- HO_q heat capacity function, W/(m² · K)
- HO_ξ sorption capacity function, kg/(m² · s)

Indices

- hyd hydraulic
- i geometric index
- j time index
- l liquid water
- s saturation
- suc suction
- v vapour
- 0 dry
- l, v vaporization.

*Thermal Insulation Laboratory, Technical University of Denmark, Building 118, DK-2800 Lyngby, Denmark.

1. INTRODUCTION

PREDICTING the moisture performance of a building construction has never been an easy task. In comparison with the calculation of temperature distributions, moisture distributions are more difficult to predict because: (1) A steady state situation hardly ever occurs. (2) The moisture transport properties of a material vary significantly with moisture content and somewhat with temperature, so the problem is non-linear. (3) There is an appreciable spread in the material properties—even within different specimens of what appears to be the same material. (4) The moisture transport is described not only by Fickian diffusion, especially in the higher moisture contents where the liquid movements are important. Convection of moist air through materials and cracks are difficult to incorporate in a calculation. (5) The flows of moisture and heat interfere on each other such that the solution of the thermal part of a problem should be accompanied by a simultaneous solution of the moisture part. (6) The boundary conditions for a calculation are not very well defined.

The problem of the non-steady behaviour of the moisture transfer, has been addressed in research that goes back to the fifties. A transient method was developed in 1958 [1] to predict the moisture content in layers of a flat concrete roof. Since then, research within the field has been ever accelerating. In more recent years, transient numerical calculation methods have been described in (to name but a few references): [2, 3, 4, 5, 6 and 7]. These models differ in their degree of sophistication. Some of them only consider vapour diffusion as the mechanism for moisture transport. A few of the models are multi-dimensional, though most are 1-D.

Models like these have been developed and used mainly within the research community. The knowledge gained from the use of the models has only been available when results of model analyses were published in reports and articles. Consultants, building designers and manufacturers in the building industry have not had access to the models themselves, and therefore the models do not constitute real design tools. In the past, for practical evaluation of the moisture behaviour of constructions, more simple analyses have been carried out based on the dew point method or Glaser's method [8]. The dew point method does not contain a calculation of the transfer of moisture, it is simply a check to compare the temperature of sensible layers with the dew point of the environment of the construction. Glaser's method considers vapour diffusion according to Fick's law using non-varying material properties and assuming steady state conditions to prevail. Both of these methods will be summarized in the sections following after introducing a roof construction that will be used throughout this article as an example for the various calculation methods.

An investigation [9], showed that out of 10 possible countries only 3 had standards for the calculation method for interstitial condensation. Five countries used the Glaser method in engineering practice though 3 more countries used the related "saturation-line/vapour-pressure-line intersection method". Only one country reported that "advanced methods" were used. Of the 10 countries, engineering practice in only 3 of them took solar gains and long wave radiation into account to formulate the boundary conditions. In seven countries, annual mean conditions were used for the boundary conditions.

2. THE CALCULATION EXAMPLE

As an example to display the merits of the different calculation methods, a flat roof construction is selected that contains some hygroscopic material. The construction is shown in Fig. 1. From the top it consists of 8 mm of roofing felt, 12.5 mm of wood fibre board, 100 mm of expanded polystyrene (EPS) and 100 mm of concrete as the supporting deck. There are two reasons why the construction has no vapour retarder: One is that in many climates it is not used for this type of construction, another is that it is desired for this purpose to see how the various methods treat the exchange of moisture between the deck and the rest of the roof which would have been hindered by the vapour retarder.

Though the construction does not have a sufficiently low U-value to conform with the Danish Building Regulations, the moderate Nordic climate of Denmark (55°N, 12°E, approximately 3000 heating degree days) and typical dwelling conditions have been chosen as the environment for the construction. Some characteristics of the environment are tabulated in Table 1.

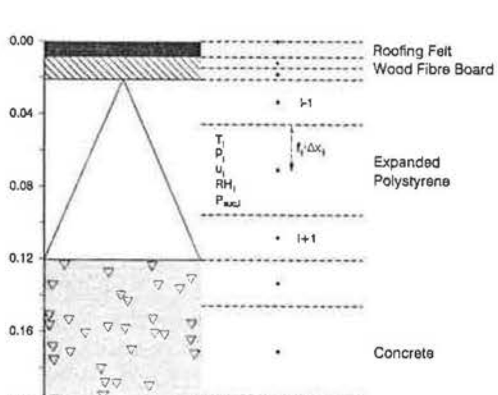

Fig. 1. Cross section of the flat roof construction used as an example for the various calculation methods and the grid used for the transient calculation.

The material properties used in these calculations to characterize the materials are tabulated in Table 2.

3. THE DEW POINT METHOD

The simplest method to control the well being of a layer which is sensible to moisture is to carry out a worst case estimate of its relative humidity. The worst case relative humidity is calculated as the ratio of the partial vapour pressure in the most humid environment of the construction to the saturation vapour pressure at the temperature of the layer, i.e. the humid air is in unobstructed contact with the material. If the material is warmer than the dew point of the surrounding air, the relative humidity at the material will be less than 100% and moisture will not condense to form free water. However, some materials like wood and steel may require that the relative humidity stays below a certain critical limit, $\varphi_{critical}$, less than 100%. Thus, the following criterion is obtained:

$$p_{surroundings} \leqslant \varphi_{critical} \cdot p_s(T_{material}). \tag{1}$$

Sometimes, $\varphi_{critical}$ may be determined by a maximum allowable moisture content in a material and its sorption curve. A safe limit for a moisture content below which wood will not suffer from biological decay is recognized to be 20% by weight [10] corresponding to $\varphi_{critical} = 85\%$. In January, when the dew point of the indoor air according to the information in Table 1 is 7.6°C, the temperature of the wood fibre board must not go below 10°C. Since the temperature of the wood fibre board will be close to that of the outdoor air (−1.0°C), the construction cannot be accepted according to this simple evaluation.

The method usually gives results very much on the safe side because an assumption inherent in it is that the vapour pressure at the sensitive layer is the same as in the most humid of the surroundings. In practice, its vapour pressure should be found somewhere between the vapour pressure of the indoor and the outdoor air, depending on the distribution of the vapour resistances among the other layers in the construction. The Glaser method, mentioned in the next section, takes the distribution of the vapour pressure into consideration.

4. GLASER'S METHOD

Glaser's method was originally a graphical method [8] developed in 1959 to determine the distribution of vapour pressures through a construction. The theory behind the method is Fickian diffusion under steady state conditions, according to which the vapour flux through a layer i in a construction may be calculated as:

$$g_{v,i} = \delta_i \frac{\Delta p_i}{\Delta x_i} = \frac{\Delta p_i}{Z_i}. \tag{2}$$

In the steady state, when there is no condensation, $g_{v,i}$ is the same throughout the construction, and Glaser used this fact to develop the graphical method. By drawing the

Table 1. Outdoor and indoor climatic conditions for a typical Danish dwelling

Month	Jan	Feb	Mar	Apr	May	Jun	Jul	Aug	Sep	Oct	Nov	Dec	Annually
Outdoor Temperature [°C]	−1.0	−0.5	1.9	5.9	10.9	15.2	16.1	15.9	12.9	8.9	4.5	0.8	7.6
Outdoor Relative Humidity [%]	92	90	86	81	77	75	80	80	83	88	90	92	84
Global Radiation [Wh/(m^2·day)]	472	1086	2277	3739	5054	6027	5071	4245	2981	1480	602	349	2790
Indoor Temperature [°C]	21	21	21	21	22	23	23	23	22	21	21	21	21.7
Indoor Relative Humidity [%]	42	40	43	51	56	56	59	62	66	61	52	46	52.8

Table 2. Hygrothermal properties for the materials in the roof construction

Material	ρ Density [kg/m^3]	Δx Thickness [mm]	λ Thermal Conductivity [W/mK]	R Thermal Resistance [m^2 K/W]	δ Vapour Permeability [kg/ms Pa]	Z Vapour Resistance [GPa m^2 s/kg]
Roofing Felt	1050	8		0.04		1400
Wood Fibre Board	300	12.5	0.055	0.23	33.0×10^{-12}	0.38
Exp. Polystyrene	20	100	0.034	2.94	5.0×10^{-12}	20
Concrete	2400	100	1.5	0.07	2.5×10^{-12}	40

width of each layer proportional to its vapour resistance instead of its geometrical thickness and plotting the vapour pressures, a straight line is obtained from one side of the construction to the other, the slope of which represents the vapour flux through each and all of the layers. The saturation vapour pressures, determined from the temperature distribution, are plotted in the same diagram. If the straight line for the vapour pressures intersects the one for saturation vapour pressures, condensation will occur in one or more points of the construction, and the vapour pressure curve is corrected such that it is tangent to the saturation curve in the condensation points and goes in straight lines below the saturation curve through the rest of the construction. The resulting change in slope of the vapour pressure curve at the condensation points reflects a difference in the flux of vapour running to and from the condensation area, i.e. the amount that condenses.

Figure 2 shows the application on the roof example of the graphical method with the Z-value plotted along the abscissa. The roof has been tilted 90 degrees in order to display an easy mnemonic way to establish the correct

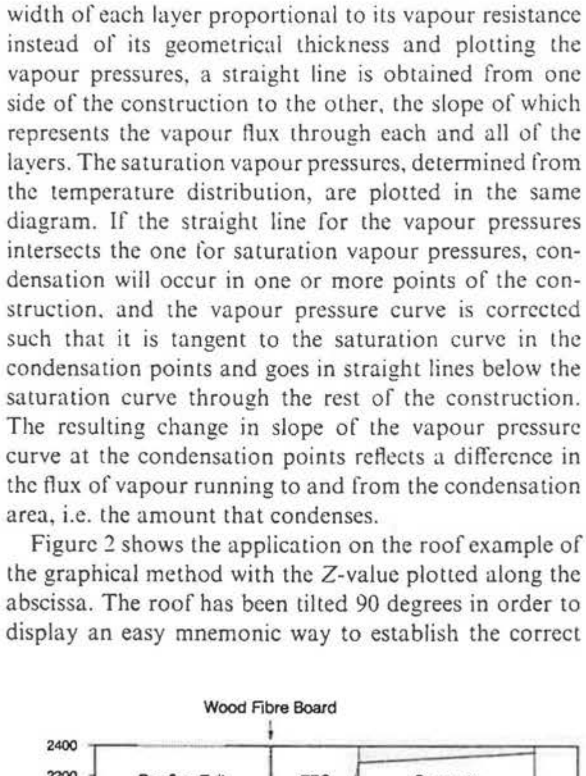

Fig. 2. Glaser's method. The vapour pressure distribution is drawn by one or more straight lines when the vapour resistances are represented by the abscissa axis.

vapour pressure curve. First, the curve for the saturation vapour pressure is drawn, and marked as the boundary of a "fixed body", impenetrable for the vapour pressure curve. The vapour pressure curve, "January (average)", is marked by a "rope" that starts out at the height of the outdoor vapour pressure on the left-hand side and ends at the height of the indoor vapour pressure on the right-hand side. Initially, the rope hangs down loosely between these two points. In order to determine the vapour pressure distribution, the rope is tightened, aiming to form a straight line between the indoor and outdoor conditions. In the attempt to do so, the rope will hit the fixed body made up by the saturation curve in the interface between roofing felt and wood fibre board where condensation is formed. The vapour pressure curve runs as a straight line to each side of the condensation point. The condensation results in a shape of the vapour pressure curve that is convex against the abscissa axis.

In periods when excess moisture is able to dry out, the Glaser method may give a prediction of the drying rate by setting the vapour pressure in the layer where the moisture is located equal to the saturation value. Under the right conditions, this will result in a shape of the vapour pressure which is concave against the abscissa axis, i.e. more vapour flows away from than to the moist layer (see "July (average)" in Fig. 3). To accept a construction, the annual drying potential must be at least as large as the annual amount of condensation, and the amount accumulated after a condensation period must not be critical by itself.

The Glaser method has been adopted by the German code DIN 4108 [11] as the proper way to verify the moisture related functionality of constructions. Even if Glaser is not accredited, similar though perhaps not graphical methods are used in most countries as the standard way to calculate the distribution and migration of moisture in building constructions (for instance [10]).

Still, the method assumes a steady state moisture transport, i.e. the adaptation of the internal moisture distribution to changes in the environment is expected to occur instantaneously. The validity of this assumption will be explored in the following sections.

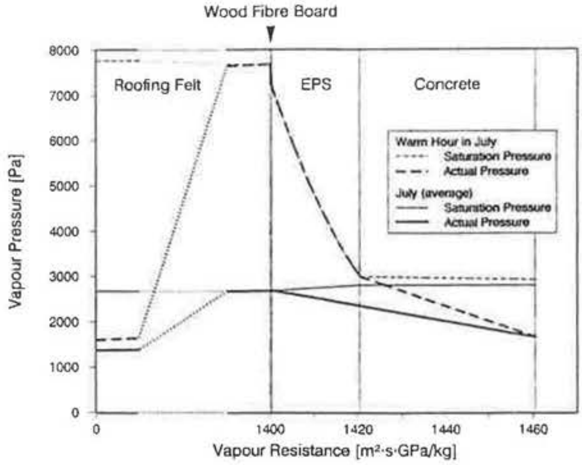

Fig. 3. Vapour pressure distributions under summer conditions.

Another question that arises when Glaser's method is used, is the selection of parameters to describe the climate that surrounds the construction. DIN 4108 [11] prescribes a climate that consists of a 60 day condensation period with outdoor conditions: -10°C and 80% RH and indoor conditions: 20°C and 50% RH. The drying period is 90 days long and has 12°C and 70% RH both indoors and outdoors. This is of course a rough simplification necessary to obtain simple design rules.

For this article, two different ways of using Glaser's method will be shown. In both cases, the indoor climate is the one described by the last two rows in Table 1. In the two cases, the outdoor climate will be described as follows:

G1. Monthly calculations. Outdoor environment described by the mean air temperature.

G2. Hourly calculation with the outdoor surface temperatures corrected for solar gain and long wave radiation.

Method G1. Monthly evaluation, average outdoor temperature. With the climatic conditions from Table 1 and indoor and outdoor surface heat transfer coefficients 7.7 and 25 W/m^2 K, respectively, a calculation of the amount stored or the potential amount dried out has been carried out. The results are listed in Table 3.

According to this method, more moisture condenses than dries out every year, and the construction should be condemned. However, since it is a roof which has a black surface, the membrane will reach high temperatures in the summer causing an increased downward movement of moisture that is not taken into account when only the monthly average outdoor temperature is used. An improvement is to incorporate a consideration of the radiative heat exchanges of the outer surface and to use shorter time intervals, such that even short, intensive temperatures peaks will be considered.

Monthly G2. Hourly evaluation, correction for radiative gains. The absorptance of the horizontal black surface is assumed to be $\alpha = 0.93$ and its emissivity $\varepsilon = 0.9$. The Danish Test Reference Year (TRY) with hourly meteorological data [12] is used to generate hourly values of outer surface temperature corrected for the radiative contributions. Among other things, the TRY contains values of outdoor temperature, dew point, solar radiation and wind speed, but not of the equivalent sky temperature used to describe the long wave heat exchange between the surface and the sky. In [13] is given an empirical expression to calculate the equivalent blackbody temperature of the sky which uses the dew point temperature to form a relation with the vapour content of the air:

$$T_{sky} = T_{out}\left[0.8 + \frac{T_{dew} - 273}{250}\right]^{1/4}. \tag{3}$$

Using a steady state approach, the surface temperature may now be calculated for each hour in the TRY as:

$$T_{surface} = \frac{\alpha E + h_{conv} T_{out} + h_{rad} T_{sky} + U^* T_{in}}{h_{conv} + h_{rad} + U^*}. \tag{4}$$

U^* is the U-value of the construction calculated from the roof surface to the indoor air. The heat transfer coefficients h_{conv} and h_{rad} are calculated as follows:

$$h_{conv} = \begin{cases} 5.82 + 3.96v\ [\mathrm{W/m^2\,K}] & v \leqslant 5\ \mathrm{m/s} \\ 7.68v^{3/4} & v > 5 \end{cases} \tag{5}$$

$$h_{rad} = \sigma\varepsilon(T_{surface}^2 + T_{sky}^2)(T_{surface} + T_{sky}) \approx \tfrac{1}{2}\sigma\varepsilon(T_{surface} + T_{sky})^3. \tag{6}$$

In order to evaluate the expression in equation (6), it is necessary that the surface temperature is known. This temperature may be determined by any of the following methods: (A) Inserting equation (6) in equation (4) and solving for $T_{surface}$. (B) The two equations may be solved by iteration, or: (C) equation (6) may be evaluated simply with the last known value for $T_{surface}$ (from the previous hour). The last method is considered sufficiently accurate for this purpose.

In some peak hours, very high temperatures may be achieved due to the absorption of solar heat. Since the vapour pressure increases still more steeply as the temperature goes up, the flow of moisture is significantly influenced by these peaks despite their short duration.

It turns out, that in some part of the summer, the (downwards) moisture flow through the EPS and the concrete are not the same. The reason is that when the roof temperature gets high, the vapour pressure curve follows the saturation curve most of the way towards the interior (see the curves for a "Warm hour in July" in Fig. 3). Due to the curvature of this curve some moisture condenses on its way through the insulation and at the top of the concrete deck. The result is a larger drying rate for the wood fibre board than for the construction as a whole.

Table 3. Condensation and potential drying in each of the months using Glaser's method with the outdoor average temperature

Month	Jan	Feb	Mar	Apr	May	Jun	Jul	Aug	Sep	Oct	Nov	Dec	Annually
Moisture Accumulation [g/m^2]	19.4	16.3	13.6	11.3	7.2	−13.3	−13.6	−11.1	6.3	14.5	16.9	19.1	86.8

Table 4. Condensation and potential drying in each of the months using Glaser's method on an hourly basis with an outdoor surface temperature that has been corrected for solar gain and long wave radiation to the sky

Month	Jan	Feb	Mar	Apr	May	Jun	Jul	Aug	Sep	Oct	Nov	Dec	Annually
Moisture Accumulation in the Wood Fibre Board [g/m^2]	21.5	14.7	11.0	−10.8	−45.2	−182.5	−172.2	−84.4	−15.9	7.2	19.0	21.6	−416.0
Moisture Accumulation in the Roof as a Whole [g/m^2]	21.5	14.9	11.2	−2.9	−14.5	−39.8	−35.6	−24.9	−3.4	11.1	19.0	21.6	−21.7

In Table 4 is shown the rate of moisture accumulation in the wood fibre board calculated by the amount that diffuses up through the EPS minus the amount that escapes through the roofing felt. Also shown is the amount of moisture accumulated by the whole of the construction calculated by the amount that diffuses up through the concrete minus the amount that escapes through the roofing felt. It is seen, that the high temperature peaks cause some very large downwards moisture fluxes that were not registered with method G1.

The use of this method requires not only that the boundary conditions have been evaluated on an hourly basis for the orientation and type of outer surface, but also that the calculation of moisture movement is carried out a large number of times. This means that the method is not manageable without the aid of a computer.

Other enhancements of Glaser's method. Another way to take the high temperature peaks into consideration without making hourly calculations is to define a reasonable number of temperature intervals and count the number of hours of the year that the surface temperature is in each interval. Now, the calculations may be performed for each interval. With this method the time scale is no longer defined, so it is not possible to say how much moisture has been accumulated by, say, the end of March. Further, since the indoor conditions vary with the time of the year, it is no longer possible to include the effect that the seasonal variation of the indoor climate has on the moisture balance with the surrounding constructions.

In the methods mentioned above, the drying was calculated as a potential maximum value which assumed that the critical layer stayed wet throughout the drying period. In reality, the moisture may dry out in the meantime such that the yearly balance between the amount condensed and dried out may be different than predicted by the calculation. There are computer programs available which keep track of the amount of moisture stored in the layers of the construction and which keep checking that this amount does not get negative [14]. Still, however, such models do not consider the building materials to be hygroscopic and therefore, the vapour pressure has either the value that corresponds to saturation conditions, or some arbitrary value, less than saturation, which depends on the boundary conditions and the distribution of vapour resistances alone. The logical solution is to associate the vapour pressure of a material with its moisture content, as it is described by the sorption curve.

5. TRANSIENT HEAT AND MOISTURE TRANSFER

5.1 *Physical assumptions*

In the following is described a 1-dimensional method to perform transient calculations of the transfer of heat, vapour and liquid moisture through composite constructions that would typically separate the indoor from the outdoor climate. The theory could be extended to multidimensional situations as well. However, this would require an additional computational effort which goes beyond the scope of this work, namely that the theory should be easy to apply in practice.

Transport processes. The transport processes in the theory to be presented involve heat conduction according to Fourier's law,

$$q = -\lambda(u, T)\frac{\partial T}{\partial x} \tag{7}$$

vapour diffusion according to Fick's law,

$$g_v = -\delta(\varphi)\frac{\partial p}{\partial x} \tag{8}$$

and liquid suction by capillary forces according to Darcy's law:

$$g_l = -K(u)\frac{\partial P_{hyd}}{\partial x} = K(u)\frac{\partial P_{suc}}{\partial x} = (KP_{suc})(u)\frac{\partial(\ln P_{suc})}{\partial x}. \tag{9}$$

No energy or mass transport by internal convection is taken into account. The rewriting of Darcy's law is made by assuming capillary forces to be the only cause of gradients in the hydraulic pressure (the numerical value of which is the suction pressure) and using the natural logarithm of the suction pressure as the driving potential. This potential and the corresponding material parameter (KP_{suc}) vary less with moisture content than their original counterparts and are therefore better suited for treatment by the numerical method introduced later. The selection of vapour and liquid pressures as the driving potentials for moisture flow is caused by a desire to have potentials that go across material boundaries in a continuous manner (this would not be the case if the moisture content were used).

The balance of specific enthalpy with respect to the dry weight, looks:

$$\rho_0\frac{\partial h}{\partial t} = \rho_0 c_p(u)\frac{\partial T}{\partial t} = -\frac{\partial q}{\partial x} - \Delta h_{l,v}\frac{\partial g_v}{\partial x}. \tag{10}$$

Inherent in this equation is an assumption that all vapour accumulating in a volume condenses to form liquid moisture and releases the heat of condensation, i.e. the mass fraction of gaseous water is negligible [15]. Of course, the opposite is true—heat is consumed—when moisture evaporates. The specific heat capacity is corrected for the moisture content in the material. The heat of formation of ice is taken into account by increasing c_p by a certain amount in a certain temperature interval

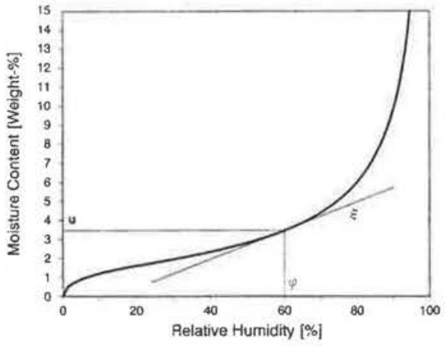

Fig. 4. Sorption curve for a hygroscopic material (cellular concrete).

below 0°C depending on the freezing point depression characteristics of the material.

The equation for the moisture balance could be written as follows, where the unindexed u designates the sum of moisture in all of the phases ice, liquid and vapour (the ice is regarded as being immobile):

$$\rho_0 \frac{\partial u}{\partial t} = -\frac{\partial g_v}{\partial x} - \frac{\partial g_l}{\partial x}. \tag{11}$$

The sorption isotherm (Fig. 4) is employed to relate the moisture content to the vapour pressure using the relative humidity and the saturation vapour pressure at the current temperature. A suction curve (Fig. 5) gives the relation between moisture content and suction pressure. Thermodynamic relations give the connection between relative humidity over the water absorbed in a porous material and the suction pressure in the liquid phase ([4], [15] and [16]), and the suction curve could therefore be represented by the sorption curve. However, the suction curve provides much more detail in the narrow region of high relative humidities (>98%), where there is still a large potential of most materials to absorb moisture in the coarse pores.

With the moisture retention curves, the left-hand side of equation (11) could be written in either of the following two ways:

$$\rho_0 \frac{\partial u}{\partial t} = \rho_0 \xi(\varphi) \frac{\partial \varphi}{\partial t} = \rho_0 \xi(\varphi) \frac{\partial \left(\frac{p}{p_s(T)} \right)}{\partial t} \tag{12}$$

$$\rho_0 \frac{\partial u}{\partial t} = \rho_0 \Xi(\ln P_{suc}) \frac{\partial (\ln P_{suc})}{\partial t}. \tag{13}$$

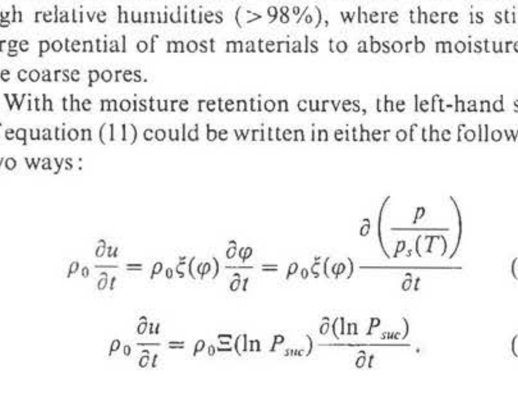

Fig. 5. Suction curve for cellular concrete.

The moisture capacities, ξ and Ξ, are the slopes of the sorption and suction curves, respectively.

Boundary conditions. The external boundary condition for heat flow is described by the following heat balance for the exterior surface:

$$\alpha E + h_{conv}(T_{out} - T) + h_{rad}(T_{sky} - T) + \Delta h_{l,v} g_v^- = q^+ + \Delta h_{l,v} g_v^+ \tag{14}$$

where the fluxes are taken to be positive in the direction from outdoors to indoors, and the superscripts − and + denote conditions on the upstream and downstream side of the boundary, respectively. The heat transfer functions may be calculated as in equations (5) and (6). The discontinuity indicated for the vapour flux is possible if the surface is impermeable or if the vapour flux in the material is parallel with a possible liquid flux, such that vapour condenses or evaporates at the surface.

The inside thermal boundary condition is treated more simply by combining the convective and radiative effects into an effective surface coefficient, h_{in}, working between the surface and the equivalent indoor temperature, T_{in}:

$$q^- + \Delta h_{l,v} g_v^- = h_{in}(T - T_{in}) + \Delta h_{l,v} g_v^+. \tag{15}$$

External and internal surface flows of vapour are calculated according to:

$$g_v = \beta \Delta p \tag{16}$$

where Δp is the vapour pressure difference between the surface and the surroundings. β is the convection mass transfer coefficient which for most conditions may be calculated from Lewis' law:

$$\beta = \frac{h_{conv}}{R_v T \rho c_p}. \tag{17}$$

On the indoor side, only the convection part of h_{in} is used to calculate β. With the exception of very wet capillary active materials or highly porous materials, the surface resistance to vapour flow will often be negligible compared with the internal resistances. Therefore, the rate of moisture exchange with the surroundings will usually be governed by the transport in the materials.

Liquid flow across the external boundaries is calculated by an external suction pressure equal to that of free water (P_{suc} negligibly small) and by having a hydraulic surface resistance, which is either zero for free water contact or infinitely large when there is no liquid flow across the boundary.

5.2 *Numerical procedure*

A Finite Control Volume (FCV) technique is used in which the construction and its material layers are divided into smaller control volumes (Fig. 1) and the time is divided into small steps of duration Δt. The geometric and the time axes are indexed with i and j, respectively. A grid point located somewhere within the control volume (not necessarily in the centre) is used to represent the value of the variables throughout the whole domain of the volume. The method keeps track of how the potentials listed in Fig. 1 are changed as a function of the heat and mass flows into and out of each control volume.

Heat transfer. Given a temperature distribution, the heat flux, q_i, conducted from control volume $i-1$ to i, may be calculated as follows:

$$q_i^{j+1} = -\frac{T_i^{j+1}-T_{i-1}^{j+1}}{\frac{(1-f_{i-1})\Delta x_{i-1}}{\lambda_{i-1}(u_{i-1}^j, T_{i-1}^j)}+\frac{f_i\Delta x_i}{\lambda_i(u_i^j, T_i^j)}+R_i}$$
$$= -H_{q,i}^j(T_i^{j+1}-T_{i-1}^{j+1}) \quad (18)$$

where R_i is a possible extra thermal resistance in the interface between layers $i-1$ and i, an air gap, for instance. The denominator of the second term represents the sum of resistances from grid point $i-1$ to grid point i. As shown in Fig. 1, f is a displacement factor used to indicate which fraction of the control volume lies on the external side of the grid point. A simpler way to write the expression is to assign one over the denominator of the second term to the heat transfer function, H_q, which is introduced in the last term.

Applying an assumption of quasi-steady conditions in a time interval, Δt, the enthalpy balance for control volume i looks:

$$\frac{\rho_{0,i}c_{p,i}(u_i^j, T_i^j)\Delta x_i}{\Delta t}(T_i^{j+1}-T_i^j) = HO_{q,i}^j(T_i^{j+1}-T_i^j)$$
$$= -(q_{i+1}^{j+1}-q_i^{j+1})-\Delta h_{l,v}(T_i^j)(g_{v,i+1}^j-g_{v,i}^j). \quad (19)$$

The heat capacity function, HO_q, is defined by the first two terms of this equation. Combination of equations (18) and (19) leads to the following equation:

$$A_{q,i}T_{i-1}^{j+1}+B_{q,i}T_i^{j+1}+C_{q,i}T_{i+1}^{j+1} = D_{q,i} \quad (20)$$

with:

$$A_{q,i} = -H_{q,i}^j$$
$$B_{q,i} = HO_{q,i}^j+H_{q,i}^j+H_{q,i+1}^j$$
$$C_{q,i} = -H_{q,i+1}^j$$
$$D_{q,i} = HO_{q,i}^jT_i^j-\Delta h_{l,v}(T_i^j)(g_{v,i+1}^j-g_{v,i}^j). \quad (21)$$

At the boundaries, $i = 1$ and $i = n$, equations (14) and (15) are modified with finite difference evaluations of the fluxes q and g and with capacity terms for the surface control volumes before they are put in the same format as equation (20). The set of equations for all i's can now be solved to find the temperature profile. The matrix of coefficients is tridiagonal, and there is an easy and rapid algorithm to solve this kind of equation system [17].

The material properties used in equations (18) and (19) are evaluated with the moisture content and temperatures at the previous time step and the heat of evaporation, $\Delta h_{l,v}$, is evaluated at the last known temperature. No attempt is made to iterate on these equations to get the material properties updated to the current time step, since it is not believed that the additional computational effort is warranted by the level of accuracy of these properties. A similar argument goes for the explicit addition of the latent heat term from the former time step.

The calculation of temperatures, as it has been described above, is carried out first in each time step because it is necessary to know the distribution of saturation vapour pressure (a direct function of temperature) before the moisture transfer is calculated.

Moisture Transfer. The transport equation for vapour diffusion is written similarly to equation (18) for conduction heat flow:

$$g_{v,i}^{j+1} = -\frac{p_i^{j+1}-p_{i-1}^{j+1}}{\frac{(1-f_{i-1})\Delta x_{i-1}}{\delta_{i-1}(\varphi_{i-1}^j)}+\frac{f_i\Delta x_i}{\delta_i(\varphi_i^j)}+Z_i}$$
$$= -H_{v,i}^j(p_i^{j+1}-p_{i-1}^{j+1}) \quad (22)$$

where Z_i is a possible extra vapour resistance in the interface between layers $i-1$ and i (a vapour retarder, for instance).

The mass conservation equation is written using the liquid moisture flux from the former time step as an explicitly added source term

$$\rho_{0,i}\Delta x_i\frac{u_i^{j+1}-u_i^j}{\Delta t} \approx \frac{\rho_{0,i}\Delta x_i\xi_i(\varphi_i^j)}{\Delta t}(\varphi_i^{j+1}-\varphi_i^j)$$
$$= HO_{v,i}^j\left(\frac{p_i^{j+1}}{p_{s,i}^{j+1}}-\frac{p_i^j}{p_{s,i}^j}\right) = -(g_{v,i+1}^{j+1}-g_{v,i}^{j+1})-(g_{l,i+1}^j-g_{l,i}^j).$$
$$(23)$$

The approximation sign between the first two expressions is used to indicate that quasi-constancy is assumed of ξ.

Combination of equations (22) and (23) gives the following equation to find a new vapour pressure distribution, p^*:

$$A_{v,i}p_{i-1}^*+B_{v,i}p_i^*+C_{v,i}p_{i+1}^* = D_{v,i} \quad (24)$$

with:

$$A_{v,i} = -H_{v,i}^j$$
$$B_{v,i} = \frac{HO_{v,i}^j}{p_{s,i}^{j+1}}+H_{v,i}^j+H_{v,i+1}^j$$
$$C_{v,i} = -H_{v,i+1}^j$$
$$D_{v,i} = \frac{HO_{v,i}^j}{p_{s,i}^j}p_i^j-(g_{l,i+1}^j-g_{l,i}^j). \quad (25)$$

A similar procedure is followed to calculate a new distribution of suction pressures using the vapour fluxes from the former time step as an explicitly added source term. Since this calculation is different from the one described above, the moisture contents may not end up exactly the same. The final step, therefore, is to regard the vapour and suction pressures marked with asterisks as intermediate results and use them in equation (22) and the similar equation for liquid transport to give the moisture fluxes g_v^* and g_l^*. These fluxes are used in a moisture balance to give the change in moisture content between time steps j and $j+1$:

$$\rho_{0,i}\Delta x_i\frac{u_i^{j+1}-u_i^j}{\Delta t} = -(g_{v,i+1}^*-g_{v,i}^*)-(g_{l,i+1}^*-g_{l,i}^*). \quad (26)$$

The new relative humidities and vapour pressures may now be determined from the sorption curve, Fig. 4, and the suction pressures could be found from the suction curve, Fig. 5.

5.3 *Application of the theory*

A model, MATCH—*Moisture and Temperature Calculations for Constructions of Hygroscopic Materials*, was developed according to the above theory [16]. The code was written for a personal computer with visual aids to improve the user-friendliness and using some of the graphical features available on these machines to display the calculation results. Since PCs are available in any office, the method may easily be adopted as a design tool.

As the program is executed, it reads the environmental data from the Test Reference Year of the particular location. Analytical expressions are used that describe the hygrothermal material properties and how they vary with temperature and moisture content. MATCH is supplied with a data base that contains parameters for these expressions for a number of building materials. It should be stressed that the acquisition of good material properties is vital for the predictions obtained with any calculation model. Today's stage of transient models has probably reached the point where the accuracy of the calculation results does not depend so much on the detailed model features as on the quality of the material properties on which the model predictions are based.

Applicability of the model. Primarily, the code applies to the analysis of constructions that separate the indoor from the outdoor climate, though other situations may be simulated. Since internal convection is not considered, and may have an important impact if it is there, the constructions must be air tight for the predictions to be valid. Sometimes, it may be assumed that the liquid transport is negligible. In order to speed up the calculations in these cases, there is an option not to consider the liquid moisture transfer.

Examples of cases that have been investigated with the model are:

- Moisture conditions in concrete and timber framed constructions. These are topics of appreciable interest from the industry, particularly concerning sloped and flat roofs.
- Drying potential of a new kind of vapour retarder, the Hygro Diode Membrane [18].
- The potential for moisture accumulation or drying through certain kinds of weather proofing membranes [16].
- Effect of latent heat transfer in wet insulation [16, 19].
- Effect of hysteresis in the moisture retention curves [16, 20].

Validation. Model predictions of the moisture distribution during drying of a homogeneous piece of cellular concrete have been successfully compared with accurate measurements with a γ-ray equipment [16, 21]. Additionally, the simulated effect of the transfer of latent heat has been compared with experimental results on flat roofs from a field test and from tests in a climate simulator, and several comparisons between MATCH predictions and measurements of moisture content in flat roofs have been carried out with satisfactory results [16]. However, when the experiments deal with composite constructions exposed to field conditions, the number of influencing parameters for the boundary conditions and the material data becomes so large that it is difficult to carry out an accurate validation. The reliability of a transient model has to lie in the experience gained over several years of its use and a continuous comparison with field results. This experience is continually built up. An annex on "Heat, Air and Moisture Transport in New and Retro-fitted Insulated Envelope Parts" within the IEA Energy Conservation in Building and Community Systems Programme [9] will investigate the combined topic of calculation models, material properties, boundary conditions and correlation with experimental results and practical knowledge.

6. DISCUSSION OF THE CALCULATION EXAMPLE

The transient calculation method was applied to the roof example, Fig. 1, to see how the transient results differ from those obtained with the simpler methods. No significant moisture transport in the liquid phase was expected to take place for the actual construction, so only the transient vapour transport was considered.

In this case, the distribution of driving potentials keeps being evaluated from the moisture content of the layers, so it was necessary to specify the magnitude of the initial moisture content. Two calculations will be shown here. One (T1) assumes the wood fibre board to be well saturated, such that the vapour pressure in the board equals the saturation value, just like it was assumed when the ratio between annual condensation and potential drying was analysed with the Glaser method. The other calculation (T2) was performed by guessing reasonable levels for the initial moisture content and simulate 10 years before running yet another year to be analysed. This eleventh year represents something close to periodic stationary conditions

Figure 6 shows the monthly and annual accumulation of moisture in the wood fibre board according to the two Glaser methods together with similar results from the two MATCH calculations. With the transient method, the accumulation is calculated by subtracting the upwards positive flux of moisture between the wood fibre board and the roof membrane from the similar flux between the insulation and the fibre board.

The monthly evaluation with Glaser's method predicts low rates of condensation in the winter and low drying rates in the summer. The reason is that this method does not consider the hygroscopic uptake of moisture by the wood in winter, and that the description of the summer drying caused by the solar heating is lacking when the average air temperature is used to describe the outer boundary conditions.

The drying rate predicted by the Glaser method with hourly time steps matches the one predicted by the tran-

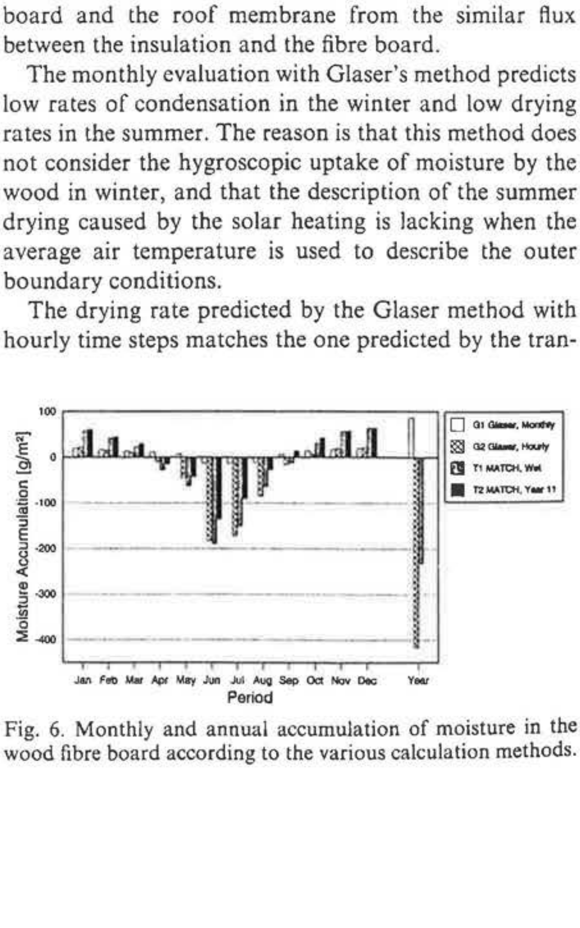

Fig. 6. Monthly and annual accumulation of moisture in the wood fibre board according to the various calculation methods.

sient method when the fibre board is saturated. However, because the Glaser method does not consider the hygroscopicity of the materials, the rate of moisture accumulation in the winter is considerably lower and, therefore, this method gives the highest annual drying rates. The transient method used under periodic stationary conditions gives slightly higher annual rates of moisture accumulation in the winter and lower drying rates in the summer than when the wood was maintained saturated. This is a result of the vapour pressures in the wood fibre board being determined by its actual level of moisture content.

Similarly, Fig. 7 shows results of moisture accumulation for the roof as a whole. The accumulation is calculated by subtracting the moisture flux between the wood fibre board and the roof membrane from the flux into the roof from the bottom. For the Glaser method with monthly evaluation, the same results are obtained as for the accumulation in the wood fibre board alone, since this is the only layer where condensed moisture is encountered with this method. The hourly evaluation of Glaser's method gives somewhat smaller drying rates in the summer than was seen for the wood fibre board alone, because some of the moisture that comes out of the wood condenses in the insulation and at the top of the concrete.

The transient method predicts accumulation rates that are in opposite phase of the Glaser results. The reason is the seasonal variation of the indoor relative humidity in combination with the hygroscopic capacity of the concrete.

The effect of the hygroscopicity is illustrated by Figs 8 and 9 which show the average vapour pressure distribution in January and July according to the Glaser methods and the MATCH calculations. While the Glaser methods have vapour pressures that follow what would be partially straight lines in the $p-Z$ diagram, the vapour pressures evaluated with the transient method are clearly influenced by the time lag. This means, that for instance the centre of the concrete is relatively more humid than its environment in the winter and relatively drier in the summer. Therefore, the moisture flux at the inside boundary is opposite of what would be expected by the steady state method. The time lag in the adaptation of the vapour pressure distribution to changes in the environment also has an impact on the vapour pressure gradients within the construction, and this is the explanation for the differences between the methods in the rates of moisture transfer to and from the wood fibre board.

As seen from Figs 6 and 7, there is a significant dis-

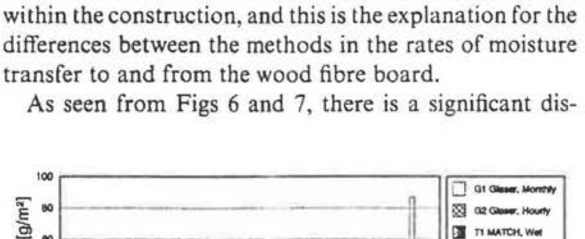

Fig. 7. Monthly and annual accumulation of moisture for the roof as a whole.

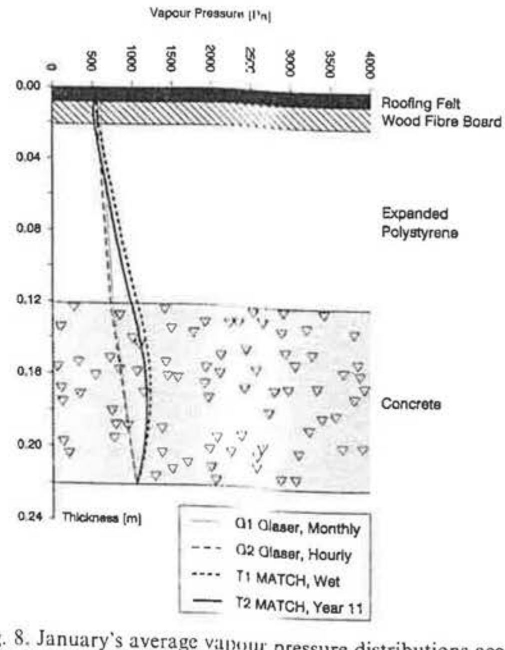

Fig. 8. January's average vapour pressure distributions according to the different calculation methods.

crepancy between the annual results obtained with the different methods. Should the design be rejected? Since the critical layer for fungal attack is the wood fibre board, its moisture content should be compared with the critical limits. Additionally, the temperature of the wood may be of importance, because of the low fungal activity at temperatures below 5°C. Figure 10 shows a plot of the daily averages of moisture content and temperature of the wood fibre board throughout the year as they were calculated with the transient method under periodic stationary conditions. The dangerous combination of temperature and moisture content, which can be defined as $T > 5$°C and $u > 20$ weight-%, is shown by a shaded background. It is seen that the moisture content gets a

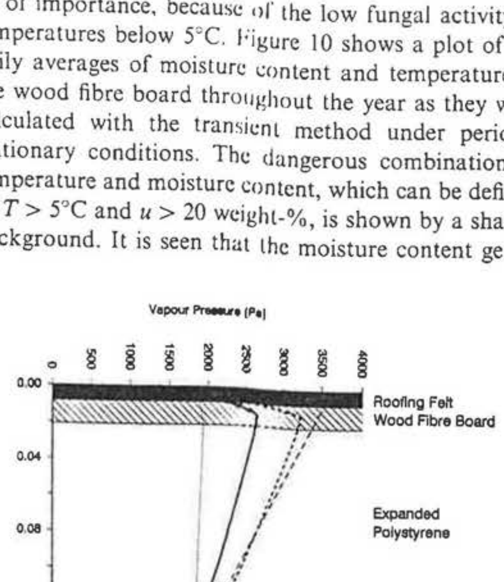

Fig. 9. July's average vapour pressure distributions according to the different calculation methods.

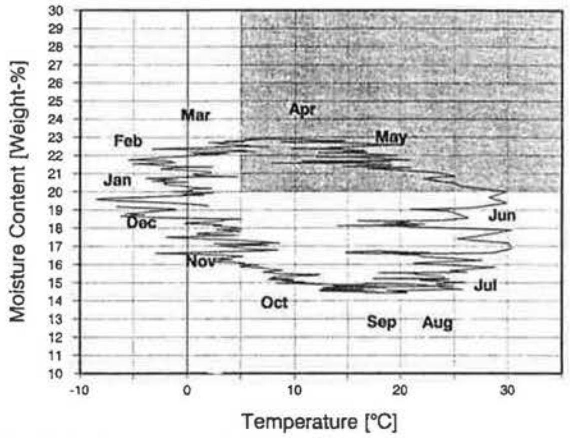

Fig. 10. Daily averages of the moisture content and temperature of the wood fibre board and the zone for potential fungal growth.

little too high in the late spring when also the temperature is so high that the fungi may grow. Though the entry into the dangerous zone is not very severe, the design should be changed towards a safer construction. Additionally, other transient calculations could have served useful to see where, for instance, construction moisture from the concrete would migrate within the first year's lifetime of the construction.

7. CONCLUSION

With finite control volume techniques, it is fairly uncomplicated to simulate combined heat and moisture transfer through building constructions in a transient way. The model presented has been used together with common non-transient calculation methods for moisture transport to compare results on a particular case, a low slope concrete roof with wood fibre board between the insulation and the roof membrane. Following is a short list of the methods and their merits:

The dew point method. The method does neither consider the distribution of vapour pressures nor the migration of moisture. The method uses the worst case of exposure to a humid environment for the sensible layers of a construction and will therefore always be on the safe side.

Glaser's method with monthly intervals in which the outdoor air temperature is used as outer boundary condition. The result is too low a rate of condensation in the wood fibre board during winter because the hygroscopicity of the materials is neglected. The drying in summer is very little because the method overlooks the drying effect on the outer layers of the solar radiation on the external surface.

Glaser's method with hourly values for the outer surface temperature considering solar irradiance and long wave radiation to the sky. Winter conditions are the same as for the previous method. The summer drying is probably too large because moisture is assumed to dry out from a saturated layer where the condensate was formed in the winter, while the full effect of the solar gain is taken into account.

Transient method with 1 hour time step in which the critical layer starts being saturated. This method simulates the same conditions for the critical layer as with the hourly Glaser method. Approximately the same drying rate in the summer is achieved. However, in the winter the rate of condensation in the wood is appreciably higher with the transient method, due to the migration of moisture deposited in internal layers of the construction towards the layer where condensation takes place.

Transient method after periodic stationary conditions have been reached. With these conditions, of course the annual accumulation is insignificant. However, due to the hygroscopic effects on the vapour pressure distribution both the patterns of internal redistribution and external exchange of moisture are significantly altered.

Other cases could have been analysed with the transient method—for instance whereto would construction moisture migrate if the construction were newly built. The method makes it possible not only to chart the pattern of moisture migration but also to follow how the moisture content of sensible layers varies with time.

The above results should be regarded as being specific to the roof construction analysed. However, it will often be such that Glaser's method without consideration of the radiative heat exchanges will give results on the safe side, i.e. too much moisture appears to accumulate. The opposite, too much moisture appears to dry out, is the result according to a radiation corrected Glaser's method because the hygroscopic inertia is neglected. A transient method is expected to give a good description of the physical phenomena taking place. Therefore, there is no safety factor in the method itself and the results depend upon the quality of material data available and on what initial and boundary conditions are used.

The transient model described in the article has been implemented in a user-friendly way on a personal computer and therefore requires no more effort of the designer to use than Glaser's method. Further information on its availability could be obtained from the author.

REFERENCES

1. I. E. Chlusov, On the Calculation of Moisture in Roof Constructions, CIB-Conference, Stockholm (1958).
2. P. I. Sandberg, Moisture Balance in Building Elements Exposed to Natural Climatic Conditions, Division of Building Technology, Lund Institute of Technology, Sweden, Report 43 (1974).
3. F. Husseini, Feuchteverteilung in porösen Baustoffen aufgrund Instationärer Wasserdampfdiffusion, Dissertation, Universität Dortmund, Germany (1982).
4. K. Kießl, Kapillarer und dampfförmiger Feuchtetransport in mehrschichtige Bauteilen, Dissertation, Universität-Gesamthochschule-Essen (1984).
5. R. Kohonen, A Method to Analyze the Transient Behaviour of Building Materials and Components. Technical Research Centre of Finland. Publications 21 (1984).

6. M. J. Cunningham, Modelling of Moisture Transfer in Structures—I. A Description of a Finite-Difference Nodal Model, *Bldg Envir.* **25**, 55–61 (1990).
7. A. Keresteciolgu, Detailed Simulation of Combined Heat and Moisture Transfer in Building Components, Proc. Thermal Performance of the Exterior Envelope of Buildings IV, ASHRAE/DOE/BTECC/CIBSE Conference, Orlando, FL (1989).
8. H. Glaser, Graphisches Verfahren zur Untersuchung von Diffusionsvorgängen, *Kältetechnik* **11**, heft 10, 345–349 (1959).
9. H. Hens, Proposal for a New Annex on Heat, Air and Moisture Transport (HAMT) in and through Highly Insulated Envelope Parts: Hygric and Energetical Consequences, Enquiry Results. International Energy Agency, Energy Conservation in Buildings and Community Systems Programme (1990).
10. American Society of Heating, Refrigerating and Air-Conditioning Engineers, ASHRAE Handbook, 1989 Fundamentals (1989).
11. Deutsches Institut für Normung, Wärmeschutz im Hochbau, DIN 4108 (1981).
12. Commission of the European Communities, Test Reference Years, TRY, Directorate General XII for Science, Research and Development (1985).
13. J. A. Duffie and W. A. Beckman, *Solar Engineering of Thermal Processes*, Wiley (1980).
14. P. Standaert, Glasta, Computer Program to Calculate Vapour Diffusion–Condensation–Drying Using an Extended Method of Glaser, Physibel, Belgium (1988).
15. A. V. Luikov, *Heat and Mass Transfer in Capillary-porous Bodies*, Pergamon Press (1966).
16. C. R. Pedersen, Combined Heat and Moisture Transfer in Building Constructions, PhD thesis, Thermal Insulation Laboratory, Technical University of Denmark, Report 214 (1990).
17. B. Carnahan, H. A. Luther and J. O. Wilkes, *Applied Numerical Methods*, Wiley (1969).
18. V. Korsgaard and C. R. Pedersen, Transient Moisture Distribution in Flat Roofs with Hygro Diode Vapor Retarder, Proc. Thermal Performance of the Exterior Envelopes of Buildings IV, ASHRAE/DOE/BTECC/CIBSE Conference, Orlando, FL (1990).
19. C. R. Pedersen, Impact of Latent Heat Transfer on the Thermal Performance of Constructions Having Vapor Permeable Insulation, Proc. Building Physics in the Nordic Countries, Trondheim, Norway (1990).
20. C. R. Pedersen, Transient Calculation of Moisture Migration Using a Simplified Description of Hysteresis in the Sorption Isotherms, Proc. Building Physics in the Nordic Countries, Trondheim, Norway (1990).
21. A. F. Nielsen, Moisture Distribution in Cellular Concrete during Heat- and Moisture Transfer, PhD thesis, Thermal Insulation Laboratory, Technical University of Denmark, Report 29 (1974).